Synthesis and properties of Au–Fe_3O_4 and Ag–Fe_3O_4 heterodimeric nanoparticles*

Ding Hao(丁 皓), Shen Cheng-Min(申承民), Hui Chao(惠 超), Xu Zhi-Chuan(徐栉川), Li Chen(李 晨), Tian Yuan(田 园), Shi Xue-Zhao(时雪钊), and Gao Hong-Jun (高鸿钧)†

Beijing National Laboratory for Condensed Matter Physics, Institute of Physics, Chinese Academy of Sciences, Beijing 100190, *China*

(Received 10 September 2009; revised manuscript received 13 December 2009)

Monodisperse Au–Fe_3O_4 heterodimeric nanoparticles (NPs) were prepared by injecting precursors into a hot reaction solution. The size of Au and Fe_3O_4 particles can be controlled by changing the injection temperature. UV–Vis spectra show that the surface plasma resonance band of Au–Fe_3O_4 heterodimeric NPs was evidently red-shifted compared with the resonance band of Au NPs of similar size. The as-prepared heterodimeric Au–Fe_3O_4 NPs exhibited superparamagnetic properties at room temperature. The Ag–Fe_3O_4 heterodimeric NPs were also prepared by this synthetic method simply using $AgNO_3$ as precursor instead of $HAuCl_4$. It is indicated that the reported method can be readily extended to the synthesis of other noble metal conjugated heterodimeric NPs.

Keywords: heterodimeric structure, monodisperse, Au–Fe_3O_4 nanoparticles

PACC: 6155F, 8110D, 8116D

1. Introduction

The controls on shape, size and composition of nanoparticles are very important in the synthesis of nanomaterials because their chemical and physical properties depend upon these factors greatly.[1−5] Noble metal and magnetic materials exhibited interesting optical and magnetic properties such as surface plasma resonance (SPR) absorption and superparamagnetism, as their size was scaled down to nanometers.[6−9] It has been found that the optical, magnetic and electronic properties of these two nanomaterials can be further varied when they are combined with each other through a nanoscale interface to form heterodimeric nanoparticles (NPs).[10−12] Because the shape and size of each component of heterodimeric NPs can be controlled separately, these heterodimeric nanoparticles show controllable bifunctional properties and thus they have been of great potential for biological sensors, magnetic resonance imaging and drug delivery.[13−15] Much effort has been devoted to the synthesis of heterodimeric NPs and various heterodimeric NPs including metal–metal oxide,[16−19] metal–metal,[17,20,21] and metal–semiconductor,[13,15,22] have been reported in recent years. These heterodimeric NPs have been successfully applied in the studies of bio-detection, drug-delivery and magneto-optical interactions,[23,24] and thus have simplified the current synthetic approaches of heterodimeric NPs, which has been desirable for their future applications.

Here, we report a simplified synthesis and the properties of monodisperse Au–Fe_3O_4 and Ag–Fe_3O_4 heterodimeric NPs. The synthesis was carried out by thermal decomposition of $Fe(CO)_5$ and reduction of $HAuCl_4$ in hot organic solvent in the presence of stabilizers. It was found that the size of Au and Fe_3O_4 particles in the heterodimeric NPs can be controlled by changing the injecting temperature of precursors. UV–Vis spectra of different sized Au–Fe_3O_4 heterodimeric NPs showed that the SPR band of the heterodimeric NPs was red-shifted compared with Au nanoparticles of similar size. The magnetization behaviours of heterodimeric NPs also exhibited a slight decrease due to the attachment of the Au component onto Fe_3O_4. This method was extended to synthesize Ag–Fe_3O_4 heterodimeric NPs by using $AgNO_3$ as precursor instead of $HAuCl_4$.

*Project supported by the National Natural Science Foundation of China (Grant Nos. 60571045 and 50872147) and the National High-Tech. Research and Development Program of China (Grant No. 2007AA03Z035).

†Corresponding author. E-mail: hjgao@aphy.iphy.ac.cn

© 2010 Chinese Physical Society and IOP Publishing Ltd

2. Experiment

2.1. Materials

Oleic acid (90%), oleylamine (70%), 1,2-hexadecandiol and 1-octadecene (90%), $Fe(CO)_5$, $HAuCl_4$ and $AgNO_3$ were purchased from Aldrich Co. Ltd. All reagents were used without further purification.

2.2. Synthesis of Au–Fe_3O_4 NPs

The synthesis process was modified based on the seed-mediated method:[16] 6 mmol oleic acid (OA), 6 mmol oleylamine (OAm), 10 mmol 1,2-hexadecandiol and 20 mL 1-octadecene (ODE) were mixed in 100 mL flask and stirred under nitrogen flow at 120 °C for 30 min. Then under a blanket of nitrogen, 0.3 mL $Fe(CO)_5$ was injected into mixed solution. After 3 min, the deaerated gold precursor solution consisting of 42 mg $HAuCl_4{\cdot}(H_2O)_3$, 0.5 mL oleylamine and 5 mL 1-octadecene was added dropwise into the hot solution within 10 min. The solution was slowly heated to 310 °C to reflux for 45 min. Then the solution was cooled down to room temperature and the heat source was removed. The solution was exposed to air for an extra hour to ensure the formation of Fe_3O_4. An amount of 40 mL of isopropanol was added into the solution and centrifuged at 8000 rpm for 10 min. The products were redispersed in hexane in the presence of 0.5 μL oleylamine and centrifuged again for 8 min at 6000 rpm. Then 40 ml ethanol was added into the solution and was centrifuged again. The Au–Fe_3O_4 NPs was dissolved in 30 ml hexane in the presence of 0.5 μL oleylamine. Furthermore, 6.0–15.8 nm Au–Fe_3O_4 NPs were prepared when precursors were injected at 160 °C.

2.3. Synthesis of 4.1–7.5 nm Ag–Fe_3O_4 NPs

1.9 mL (6 mmol) oleic acid, 2.0 mL (6 mmol) oleylamine, 10 mmol 1,2-hexadecandiol and 20 mL 1-octadecene were mixed in a 100 mL flask. The mixed solution was heated to 120 °C under nitrogen gas flow for 30 min. At stirring, 0.3 mL $Fe(CO)_5$ solution was injected into this mixed solution. After 5 min, the deaerated silver precursor solution consisting of 35.2 mg $AgNO_3$, 1.0 mL oleylamine and 5.0 mL toluene solution was added to the hot solution. The solution was heated to 205 °C to reflux for 90 min. Then the solution was cooled down to room temperature and the heat source was removed. The solution was exposed to air for an extra hour to ensure the formation of Fe_3O_4. Forty mililiters of isopropanol was added to the solution and centrifuged at 8000 rpm for 10 min. The products were redispersed in hexane in the presence of 0.5 μL oleylamine and centrifuged for 8 min at 6000 rpm. The products were finally dissolved in 30 ml hexane in the presence of 0.5 μL oleylamine.

2.4. Characterization of Au–Fe_3O_4 NPs

The morphology of the product was characterized by a Philips EM-420 transmission electron microscope (TEM) at an acceleration voltage of 120 kV. UV–Vis absorption spectra were obtained using a Perkin Elmer Lambda 35 UV/Vis spectrometer. The magnetic properties of samples were examined by a Lakeshore 7404 high sensitivity vibrating sample magnetometer (VSM) with fields up to 1.5 Tesla at room temperature. The x-ray diffraction (XRD) patterns were collected on a Bruker AXS D8-advanced diffractometer with Cu Kα radiation (= 1.5418 Å, 1 Å = 0.1 nm).

3. Results and discussion

The monodisperse Au–Fe_3O_4 NPs with different sizes were synthesized at different injection temperatures of precursors. The TEM images of Au–Fe_3O_4 NPs are shown in Fig. 1. It can be seen that the size of Au–Fe_3O_4 NPs can be controlled by changing the injection temperature of $Fe(CO)_5$ and $HAuCl_4$. The 7.4 $\pm$ 1.3 nm Au–12.1 $\pm$ 1.6 nm Fe_3O_4 (Fig. 1(a)) and 6.0 $\pm$ 0.82 nm Au–15.8 $\pm$ 2.4 nm Fe_3O_4 (Fig. 1(b)) were obtained by injecting precursors at 120 °C and 160 °C, respectively. The Au–Fe_3O_4 heterodimeric NPs show narrow size and shape distributions. The standard deviations of Au and Fe_3O_4 are 12%–18% and 23%–30%, respectively. The size of Au NPs decreases and that of Fe_3O_4 NPs increases as the injecting temperature of precursors increases. The Au particles appear darker and Fe_3O_4 are light coloured in the image because Au has a higher electron density.[16] These results differ slightly from Sun's report, in which the size of Au in the heterodimeric NPs increased with increasing injecting temperature of $HAuCl_4$. The main reason should be ascribed to the difference between the two injection processes of $HAuCl_4$. Sun *et al.*[16] injected

$HAuCl_4$–OAm–ODE solution rapidly into the hot solution at different temperatures to tune the size of Au particles.

In our experiment, we added $HAuCl_4$–OAm–ODE solution dropwise into the hot solution within 10 min. When Au precursor solution was slowly dropped into the solution, Au^{3+} ions were reduced to small Au^0 clusters, which can be seeds for further growth of Au crystals. With Au precursor solution dropped gradually, Au^{3+} ions can adsorb on the seeds to grow large Au particles. At a higher injection temperature (160 °C), the increase of reduction rate of Au^{3+} ions will lead to the decrease of size of Au particles.

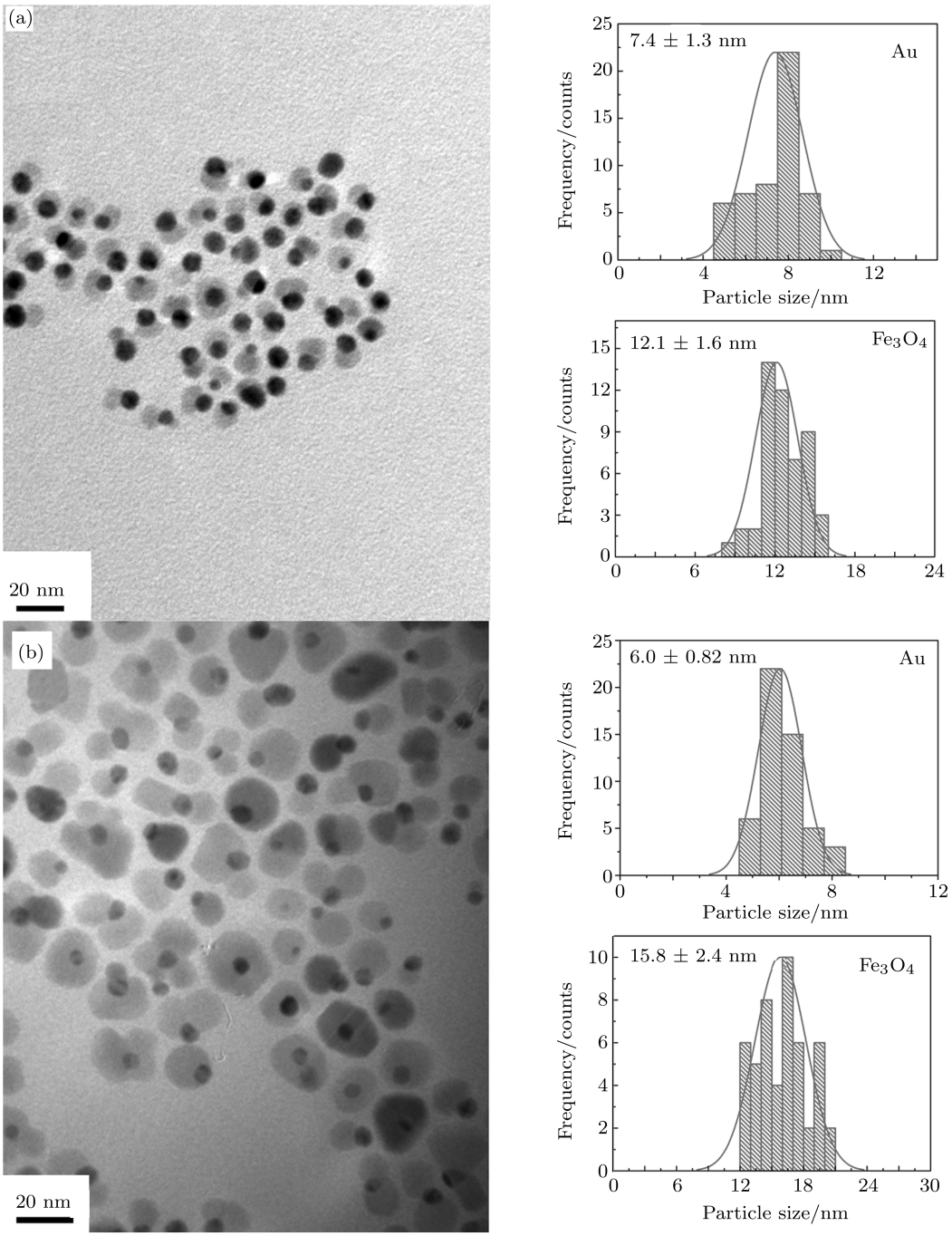


Fig. 1. TEM images and size distribution histograms of Au–Fe_3O_4 NPs prepared at different injection temperatures of precursors: (a) 7.4 ± 1.3 nm Au–12.1 ± 1.6 nm Fe_3O_4 at 120 °C; (b) 6.0 ± 0.82 nm Au–15.8 ± 2.4 nm Fe_3O_4 at 160 °C.

As shown in Fig. 2, the typical XRD pattern of the Au–Fe_3O_4 (6.0–15.8 nm) heterodimeric NPs shows the main reflection peaks of Au and Fe_3O_4, indicating that the heterodimeric NPs are indeed composed of Au and Fe_3O_4. The diffraction peaks of Au and Fe_3O_4 are consistent with the standard ones of Au (JCPDF 04-0784) and Fe_3O_4 (JCPDF 88-0866). The results prove that the components of heterodimeric NPs are face-centred cubic structure of Au and cubic spinel structure of Fe_3O_4.

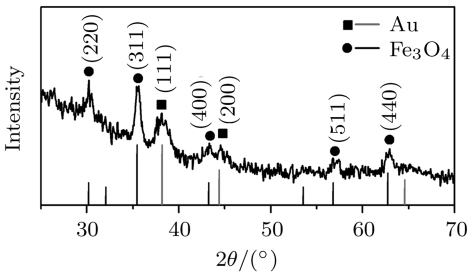


Fig. 2. The typical XRD pattern of Au–Fe_3O_4 (6.0–15.8 nm) NPs. The reflection peaks of Au and Fe_3O_4 in the heterodimeric NPs match well with the standard ones of Au (JCPDF 04-0784) and Fe_3O_4 (JCPDF 88-0866).

The UV–Vis spectrum of Au–Fe_3O_4 heterodimeric NPs dispersed in hexane solution is shown in Fig. 3. Compared with the absorption spectrum of 7 nm Au NPs (at 525 nm), the SPR bands of Au parts in the heterodimeric NPs are evidently red-shifted. The SPR band of 7.4–12.1 nm Au–Fe_3O_4 NPs and that of 6.0–15.8 nm Au–Fe_3O_4 NPs are located at 545 nm and 540 nm, respectively. The position and width of the SPR band also change due to the size difference of Au particles in heterodimeric NPs. When the size of Au particles in heterodimeric NPs becomes small, the SPR band is blue-shifted and the absorption peak becomes broader. This is confirmed by the fact that the size of Au particles in Au–Fe_3O_4 heterodimeric NPs has influence on the SPR band of the heterodimeric NPs.

The hysteresis loops of heterodimeric NPs prepared at different injecting temperatures of the precursors are shown in Fig. 4. Au–Fe_3O_4 NPs show superparamagnetic characteristics at room temperature (300 K). It can be seen from Fig. 4 that the saturation magnetization of Au–Fe_3O_4 NPs decreases compared with pure Fe_3O_4 NPs. The saturation magnetization of Au–Fe_3O_4 NPs prepared at 160 °C injection temperature is higher than that prepared at 120 °C. This is because the size of Fe_3O_4 particles in the heterodimeric NPs prepared at 160 °C is bigger and the mass percentage of the Fe_3O_4 component is relatively higher than that prepared at 120 °C. This is consistent with the reports of other research groups.[16]

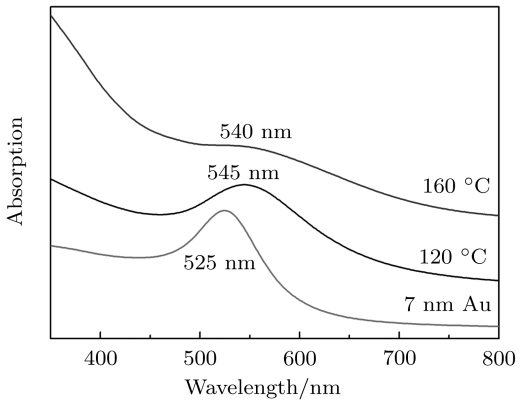


Fig. 3. UV–Vis spectra of Au–Fe_3O_4 NPs prepared at different injection temperatures of precursors. The SPR bands of 7.4–12.1 nm Au–Fe_3O_4 NPs and 6.0–15.8 nm Au–Fe_3O_4 NPs are located at 545 nm and 540 nm, respectively. Compared with 7 nm Au, the SPR band of Au–Fe_3O_4 NPs is evidently red-shifted.

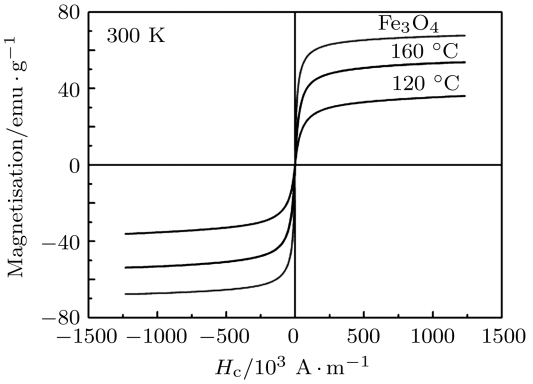


Fig. 4. The room-temperature hysteresis loops of Au–Fe_3O_4 NPs prepared at different injection temperatures of precursors. Au–Fe_3O_4 heterodimeric NPs show superparamagnetic characteristics at room temperature.

Under similar reaction conditions, we also successfully prepared Ag–Fe_3O_4 heterodimeric NPs using $AgNO_3$ instead of $HAuCl_4$ as precursor at 220 °C. Figure 5(a) shows a typical TEM image of the as-prepared Ag–Fe_3O_4 heterodimeric NPs. These Ag–Fe_3O_4 NPs are in good monodispersity and the sizes of Ag and Fe_3O_4 particles are 4.7 ± 0.9 nm and 2.8 ± 0.4 nm, respectively. The SPR absorption of Ag–Fe_3O_4 NPs is at around 421 nm as shown in Fig. 5(b), in which the peak is red-shifted by 12 nm away from that of the pure Ag NPs of similar size. The hysteresis loop of Ag–Fe_3O_4 NPs shows that the heterodimeric NPs are superparamagnetic at room temperature. Their saturation magnetization is 9.5 emu/g, which is much lower than that of pure Fe_3O_4 NPs due to the relatively low mass percentage of Fe_3O_4 component in these heterodimeric NPs.

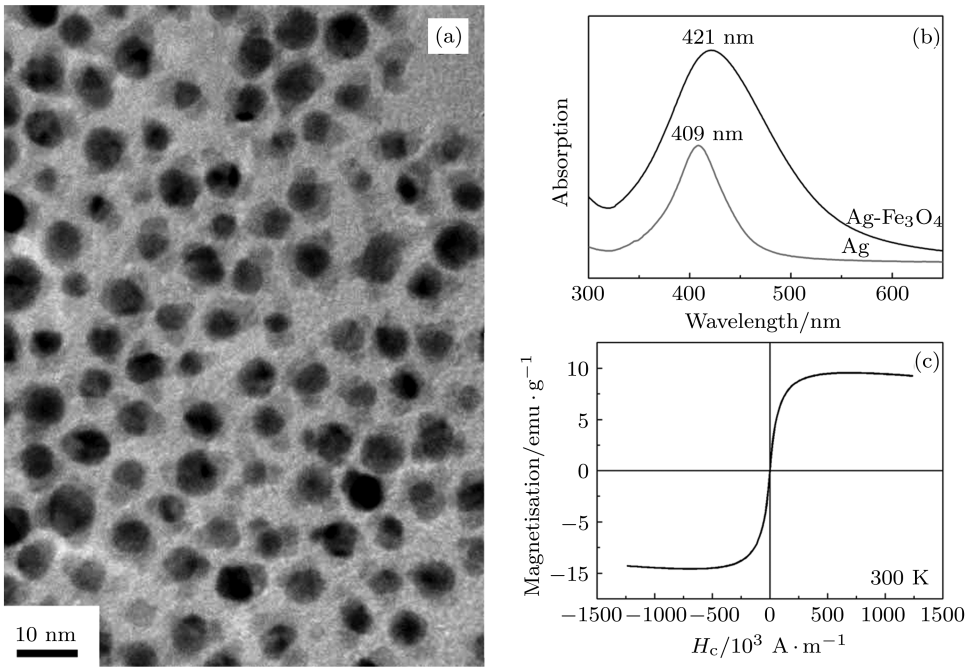


Fig. 5. The typical TEM image (a), the UV–Vis spectrum (b) and the room-temperature hysteresis loop of 4.7 nm Ag–2.8 nm Fe_3O_4 NPs. Ag–Fe_3O_4 NPs are dispersed well in non-polar solvents and the SPR band is red-shifted compared with that of the Ag NPs with similar size. The saturation magnetization of these Ag–Fe_3O_4 NPs decreases significantly due to the relatively low mass percentage of Fe_3O_4 component.

4. Conclusions

Monodisperse Au–Fe_3O_4 and Ag–Fe_3O_4 heterodimeric NPs with different sizes were prepared via the thermal decomposition of $Fe(CO)_5$ and the reduction of $HAuCl_4$ or $AgNO_3$. Different materials of 7.4 ± 1.3 nm Au–12.1 ± 1.6 nm Fe_3O_4 and 6.0 ± 0.82 nm Au–15.8 ± 2.4 nm Fe_3O_4 were prepared when the injection temperatures of precursors were 120 °C and 160 °C, respectively. The XRD pattern of Au–Fe_3O_4 NPs shows that the NPs consist of fcc Au and cubic spinel structured Fe_3O_4. UV–Vis spectra of NPs show that the SPR bands of Au–Fe_3O_4 heterodimeric NPs were evidently red-shifted compared with pure 7 nm Au particles. The hysteresis loops of Au–Fe_3O_4 and Ag–Fe_3O_4 heterodimeric NPs indicate that they are superparamagnetic at room temperature with a relative decrease in the saturation magnetization. The reported synthetic method offers an easy way to control two components of heterodimeric NPs and should be applicable to the size-controlled synthesis of other heterodimeric NPs.

References

[1] Shevchenko E V, Talapin D V, Kotov N A, O'Brien S and Murray C B 2006 *Nature* **43** 955

[2] Lu A H, Salabas E L and Schth F 2007 *Angew. Chem. Int. Ed.* **46** 1222

[3] Xiao C W, Shen C M, Xu Z C, Yang T Z and Gao H J 2008 *Chin. Phys.* B **17** 2066

[4] Shen C M, Yang T Z, Xiao C W, Zhang H R, Tian J F, Bao L H, Li C, Li J Q and Gao H J 2008 *Chin. Phys.* B **17** 2191

[5] Wang K, Yang G, Long H, Li Y H, Dai N L and Lu P Y 2008 *Acta Phys. Sin.* **57** 3862 (in Chinese)

[6] Shen C M, Hui C, Yang T Z, Xiao C W, Chen S T, Ding Hao and Gao H J 2008 *Chin. Phys. Lett.* **25** 1479

[7] Shen C M, Hui C, Yang T Z, Xiao C W, Tian J F, Bao L H, Chen S T, Ding H and Gao H J 2008 *Chem. Mater.* **20** 6939

[8] Xu Z C, Shen C M, Hou Y L, Gao H J and Sun S 2009 *Chem. Mater.* **21** 1778

[9] He S T, Yao J N, Jiang P, Shi D X, Zhang H X, Xie S S, Pang S J and Gao H J 2001 *Langmuir* **17** 1571

[10] Gu H W, Zheng R K, Zhang X X and Xu B 2004 *J. Am. Chem. Soc.* **126** 5664

[11] Frey N A, Phan M H, Srikanth H, Srinath S, Wang C and Sun S 2009 *J. Appl. Phys.* **105** 07B502

[12] Steiner D, Mokari T, Banin U and Millo O 2005 *Phys. Rev. Lett.* **95** 056805
[13] Lin X M and Samia A S 2006 *J. Magn. Magn. Mater.* **305** 100
[14] Cho S J, Jarrett B R, Louie A Y and Kauzlarich S M 2006 *Nanotechnology* **17** 640
[15] Huang Y F, Huang K M and Chang H T 2006 *J. Colloid Interf. Sci.* **301** 145
[16] Yu H, Chen M, Rice P M, Wang S X, White R L and Sun S 2005 *Nano Lett.* **5** 379
[17] Gu H W, Yang Z M, Gao J H, Chang C K and Xu B 2005 *J. Am. Chem. Soc.* **127** 34
[18] Zhang L, Dou Y H and Gu H C 2006 *J. Colloid Interf. Sci.* **297** 660
[19] Li Y Q, Zhang Q, Nurmikko A V and Sun S 2005 *Nano Lett.* **5** 1689
[20] Choi J S, Jun Y W, Yeon S I, Kim H C, Shin J S and Cheon J W 2006 *J. Am. Chem. Soc.* **128** 15982
[21] Pellegrino T, Fiore A, Carlino E, Giannini C, Cozzoli P D, Ciccarella G, Respaud M, Palmirotta L, Cingolani R and Manna L 2006 *J. Am. Chem. Soc.* **128** 6690
[22] Shi W L, Zeng H, Sahoo Y, Ohulchansky T Y, Ding Y, Wang Z L, Swihart M and Prasad P 2006 *Nano Lett.* **6** 75
[23] Xu C J, Wang B D and Sun S 2009 *J. Am. Chem. Soc.* **131** 4216
[24] Xu C J, Xie J, Ho D, Wang C, Kohler N, Walsh E G, Morgan J R, Chin Y E and Sun S 2008 *Angew. Chem. Int. Ed.* **47** 173